Numerical Simulation of Hit Noise Generation Due to Sloshing Phenomenon in a Rectangular Tank Under Periodic Excitation

Siva Teja Golla
Department of Mechanical and Aerospace Engineering,
Indian Institute of Technology Hyderabad,
Sangareddy, Telangana 502285, India

Atul R. Jadhav
Department of Mechanical and Aerospace Engineering,
Indian Institute of Technology Hyderabad,
Sangareddy, Telangana 502285, India

Raja Banerjee
Department of Mechanical and Aerospace Engineering,
Indian Institute of Technology Hyderabad,
Sangareddy, Telangana 502285, India

B. Venkatesham[1]
Department of Mechanical and Aerospace Engineering,
Indian Institute of Technology Hyderabad,
Sangareddy, Telangana 502285, India
e-mail: venkatesham@mae.iith.ac.in

Sloshing in fuel tanks is one of the major sources of noise in hybrid and high-end vehicles. During sloshing, the fluid causes impacts on tank walls resulting in their vibration, which further leads to noise, referred to as "hit noise." Therefore, hit noise generation is a multi-physics phenomenon involving fluid flow, structural response, and acoustic radiation. This paper presents a multi-physics approach to predict hit noise in a rectangular tank. The methodology involves the prediction of fluid loading on tank walls and their structural response using transient fluid and structural analyses which are weakly coupled. Radiated hit noise is predicted using acoustic finite element analysis. Longitudinal periodic excitation is applied to the fluid domain at different frequencies to simulate the sloshing regime which has dominant fluid–structure interactions. Parameters like tank wall pressures, the resulting dynamic acceleration, and radiated sound pressure levels are monitored and validated with the experimental results available in the literature.
[DOI: 10.1115/1.4056208]

1 Introduction

In recent times, in hybrid and high-end vehicles, the noise from conventional sources like engine, transmission system, etc., have been lowered. Due to this, previously subdued noises became noticeable. Sloshing noise from the fuel tank is one such kind of noise. It occurs predominantly during acceleration/braking of the vehicle and can affect the qualitative perspective of the vehicle by the passengers. Thus, reducing this sloshing noise from fuel tanks has become a new challenge to automotive original equipment manufacturers. This requires a proper understanding of the sloshing noise generation and an appropriate prediction of the sound radiated from the tank during the design phase.

Sloshing noise is generated in partially filled tanks due to the interaction of the fluid with the surrounding structures and fluids, under the influence of external excitations due to the driving conditions of the vehicle [1]. Based on the interaction of the fluid in the tank, Wachowski et al. [2] classified the sloshing noise into structure-borne and fluid-borne noises. Noise generated due to the interactions of the fluid with the tank walls is structure-borne and is referred to as hit noise, whereas, fluid–fluid interactions result in "splash noise." Prediction of these noises in the design stage would help in incorporating the appropriate noise control solutions and also reduce potential delays in product development. As the generation mechanism is different, the prediction methodologies for hit and splash noises are also different. This paper focuses on the development of prediction methodology for the hit noise only.

During the fluid–structure interactions, the dissipation of fluid energy occurs on the tank walls for a short duration of time. This often imposes impact loading on the tank walls leading to vibrations, which further induce vibrations into the surrounding medium causing hit noise. Thus, it can be understood that the generation of sloshing noise is highly dependent on the fluid motion inside the tank.

Ibrahim [1] has classified the fluid motion during sloshing into planar, nonplanar, and chaotic regimes, based on the shape of the fluid-free surface. Planar regime is characterized by the free surface which is plane in shape and undergoes low amplitude oscillations. In the nonplanar regime, the fluid motion is characterized by the presence of hydraulic jumps. They lead to fluid–structure interactions which cause the dissipation of fluid energy on the tank walls. This results in the elevation of the liquid column along the tank walls. The chaotic regime, based on the strength of excitation, is characterized by interactions which are either fluid–structure dominant (or) fluid–fluid dominant. At the excitations closer to sloshing resonance, the chaotic regime is characterized by the presence of fluid–structure interactions and wave breakages. After this stage, as the excitations become even stronger, the interactions in the chaotic regime get transformed from fluid–structure dominant to fluid–fluid dominant [3]. Therefore, it can be understood that the hit noise occurs predominantly in the nonplanar and chaotic regimes and its magnitude depends on various factors like shape of the tank, fill level, excitation, etc. Thus, the prediction of hit noise during sloshing is reliant on the accuracy of simulating the fluid flow in a container, loading on the tank walls, and its structural response.

A good amount of work related to the numerical analysis of sloshing is reported in the open literature. It includes the study of fluid flow, estimation of free surface elevation, and fluid loading along the tank walls in the containers of different geometries, under various types of excitations. Rebouillat and Liksonov [4] reviewed different numerical methods adapted to simulate the sloshing phenomenon for various industrial applications. This includes the effect of different geometries of containers, various types of excitations, the presence of different types of baffles, etc., Chen and Xue [5] used OPENFOAM to study the effect of fill level on tank wall pressures under the influence of longitudinal periodic excitation and validated with the experiments. The effect of fill level on the hard-spring and soft-spring nature of the fluid during the sloshing phenomenon is clearly understood. Baffles are used inside the tank to control the fluid motion and thus, reduce the

[1]Corresponding author.

Contributed by the Fluids Engineering Division of ASME for publication in the JOURNAL OF FLUIDS ENGINEERING. Manuscript received December 5, 2021; final manuscript received November 5, 2022; published online December 9, 2022. Assoc. Editor: Ning Zhang.

loading on the tank walls. Eswaran et al. [6] employed volume-of-fluid (VOF) method along with the arbitrary Lagrangian–Euler technique to numerically simulate the sloshing in a rectangular tank with horizontal and vertical baffles. The tank wall pressures are monitored under the influence of longitudinal periodic excitations and validated with the experiments. It is observed that the presence of baffles has reduced the fluid loading on tank walls. Vaishnav et al. [7] developed a VOF-based CAE methodology which predicts tank wall pressures and free surface shape during sloshing under braking. These monitored quantities are correlated with the experimentally measured sloshing sound pressure levels and the effect of various parameters like wall reference pressure location, free surface courant number, etc., are studied. Liu et al. [8] have given a comparison of different turbulence models for the simulation of sloshing motion. With experimental validation, it is proven that the choice of an appropriate turbulence model has a significant effect on the free surface profiles and tank wall pressures. Kabiri et al. [9] investigated the surface wall forces induced onto the tank walls during the fluid impacts in a rectangular tank. This is done through the Lattice Boltzmann-based numerical simulations. The numerical solutions are qualitatively and quantitatively validated with the experiments in terms of the free surface profile of the fluid, and dynamic pressures on the tank wall in time and frequency domains. Extensive work related to the numerical studies on sloshing and the effect of various parameters on it, like the presence of baffles, etc., has been reported in the open literature [10–18].

However, a limited amount of work has been done in the perspective of simulating the radiation of noise due to sloshing. De Man et al. [19] presented the effect of sloshing noise at the driver's ear in a car through objective and subjective studies. These studies are done with an actual fuel tank that is fixed to the car under braking excitation for different fill levels, under both on and off conditions of the engine. These results are given in terms of the sound pressure levels and annoyance rating of the driver. It is understood from these results that when the engine is on, the sloshing noise is significant at the initial stages immediately after the braking. Later it gets masked under the engine noise. When the engine is in off condition, like in the case when a hybrid car is running on battery, the sloshing noise is clearly noticeable at the driver's position and is annoying. Several automotive original equipment manufacturers are actively working to understand various aspects of the sloshing noise like the source mechanism, path control, and sound quality at receiver [2,20,21].

Park et al. [22] studied the effect of factors like baffles, mounting pads, stiffness of the tank, and amount of fuel on the tank wall vibrations using the FSI analysis. A correlation is identified between the effect of each of these parameters on the tank wall vibrations and the measured sound pressure levels due to sloshing. Roh et al. [23] predicted the pressure gradients on the tank walls numerically, under acceleration excitation for different shapes of the tank and aspect ratios. No correlation is identified between the monitored pressure gradients on the tank walls and the measured sloshing noise. Fan Li et al. [24] predicted the sloshing noise radiated from a fuel tank under braking excitation. The tank wall vibration due to fluid loading is predicted using structural and CFD solvers and the vibration response is imposed as a boundary condition to the acoustic domain. The predicted sound pressure levels are subjectively evaluated with the vehicle tests, for different fill levels. It is understood that the mean kinetic energy is not a reliable parameter to predict the slosh noise performance of a fuel tank.

It is understood from the literature that most of the numerical studies on sloshing noise have focused on correlating the measured sound pressure levels with the predicted fluid (or) structural vibration parameters under braking excitation. Braking causes both fluid–structure and fluid–fluid interactions in quick successions. This leads to the occurrence of both hit and splash noises simultaneously. This could result in improper assessment of the sloshing sound levels when correlated with other parameters. Thus, there is a need to develop controlled conditions to separately study the underlying physics behind the generation of hit noise, which is the focus of this paper. Also, a numerical analysis that demonstrates the effect of various sloshing dynamic events on the radiated noise, with proper validation is required.

The flow conditions for hit noise generation are emulated by imposing longitudinal periodic excitation in terms of sloshing natural frequency. Braking/impulse excitation can be expressed as a summation of multiple periodic excitations. In view of this, authors developed a multi-physics methodology to predict the hit noise radiated from the tank under longitudinal periodic excitation. Also, the excitation amplitude is chosen in a way to match the typical deceleration of the passenger cars under normal driving conditions, i.e., between 1 and 3 m/s^2 [25,26].

Through this, only the noise generation due to fluid–structure interactions can be predicted using the vibro-acoustic model. This prediction model helps in understanding the hit noise generation mechanism and also its contribution to the overall sloshing noise. Due to the transient nature of the fluid flow inside the tank, the proposed methodology adopts time-domain analysis across all three physical domains—fluid, structural, and acoustics. This could give an insight into the appropriate simulation of fluid motion, its interaction with the surrounding structures, and the radiation of sound.

The multi-physics methodology proposed in this paper incorporates a weakly coupled fluid–structure interaction model and a transient acoustic analysis. This work's emphasis is on the simulation of hit noise radiation for different fill levels. For this, a fluid flow regime with dominant fluid–structure interactions has to be emulated. This is done by imposing longitudinal periodic excitation on the fluid domain, at frequencies close to the sloshing resonance (f_s) [27]. Parameters like fluid free surface, tank wall pressures, displacement of the tank wall, and radiated sound pressure levels are predicted and compared with the experiments.

2 Experimental Setup

A rectangular tank of dimensions $0.238 \times 0.22 \times 0.238\,m(L \times H \times B)$ and wall thickness (t) of 0.006 m is considered for the study, which is the same as in Refs. [3] and [27]. Different sloshing regimes can be created inside the partially filled tank by imposing periodic excitation at different frequencies through a reciprocating test setup, which is shown in Fig. 1. For a given fill level, a regime of dominant fluid–structure interactions is created by imposing a longitudinal periodic excitation at the frequencies close to the sloshing natural frequency (f_s) which is given by

$$f_s = \frac{1}{2\pi}\sqrt{g k_n \ \tan h(k_n h)} \tag{1}$$

where k_n is $(2n-1)\pi/L$ for asymmetric modes and $2n\pi/L$ for symmetric modes, f_s is sloshing natural frequency, L is the dimension of the tank in the direction of excitation (m), h is depth of fluid in the tank (m), and g is acceleration due to gravity (m/s^2). The excitation frequencies of $0.75f_s$ and $1f_s$ are chosen to create a regime of dominant fluid–structure interactions [3].

For the given fill level, the loading on the tank walls due to fluid–structure interactions is measured in the dynamic pressure and acceleration using respective dynamic sensors. As the dynamic events during the sloshing take place close to the fluid free surface [1], these sensors are positioned at a level of $0.1H$ below the free surface, on front and rear tank walls as in Refs. [3] and [27]. At this level, the dynamic pressure sensor is flush mounted at the center of the wall and the accelerometer is attached adjacent to it as shown in Fig. 2. The radiated sound is measured using the microphones positioned at a distance of 1 m from the front tank wall, as shown in Fig. 1. The fluid flow during sloshing is captured using a high-speed camera at a rate of 1000 fps. The acceleration of the carriage is measured using an inertial accelerometer which is fixed to the carriage. All these measured

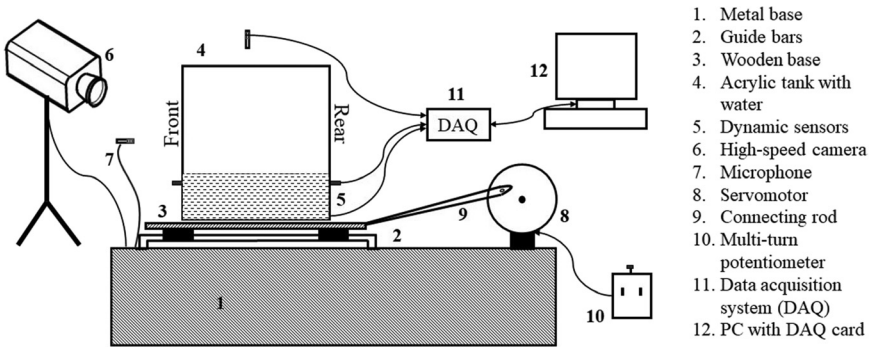

Fig. 1 Schematic of reciprocating test setup for sloshing noise measurement

parameters are useful to validate the numerical methodology for predicting the sloshing noise.

3 Numerical Methodology

Figure 3 shows the flowchart of the proposed multi-physics numerical methodology adopted to simulate the hit noise. In this, the fluid and structural domains are weakly coupled. In this weak coupling, the pressure on the tank walls due to fluid interactions is transferred to the structural domain as a loading condition and the tank wall displacements due to this pressure loading are transferred to the fluid domain as a new boundary condition. This exchange process is done at every time-step. The tank wall vibrations obtained in the form of displacements are applied as a boundary condition to the acoustic domain in the transient FEM analysis. The details of the analysis in each physical domain are given below.

3.1 Fluid Analysis. Sloshing in partially filled tanks is a two-phase flow phenomenon involving liquid and air. This requires solving the governing equations of the fluid flow—mass and momentum conservation equations with the no-slip wall boundary conditions. For different excitation frequencies, the inertial acceleration measured during the experiments is used as a longitudinal acceleration component in the numerical fluid analysis. This helps in simulating the fluid flow similar to that in the experiments. The variation of the inertial acceleration for 20% fill level at $1f_s$ excitation and the schematic of the fluid domain in the numerical analysis are shown in Figs. 4(*a*) and 4(*b*), respectively.

The fluid flow during sloshing is often turbulent and the average time behavior of these flows is of practical interest. Thus, the governing equations are to be time-averaged assuming that the fluctuations are rapid and random about the mean value. The motion of an incompressible fluid in a tank is governed by time-averaged mass and momentum conservation equations as given by Eq. (2)

$$\frac{\partial \overline{u_i}}{\partial x_i} = 0 \tag{2a}$$

$$\frac{\partial \overline{u}_i}{\partial t} + \frac{\partial \overline{u}_i \overline{u}_j}{\partial x_j} = \frac{-1}{\rho}\frac{\partial \overline{p}}{\partial x_i} + \frac{\partial}{\partial x_j}\left[\frac{\mu}{\rho}\left(\frac{\partial \overline{u}_i}{\partial x_j} + \frac{\partial \overline{u}_j}{\partial x_i}\right) - \tau_{ij}\right] + f_i \tag{2b}$$

where $\overline{u}_i$ and $\overline{p}$ are the time-averaged velocity component and pressure, ρ is the density of the fluid, μ is the viscosity, τ_{ij} is the turbulent stress tensor, and f_i is the body force component.

The fluid interface in a two-phase flow is traced using the VOF model. The presence of fluid interface in a cell is indicated by its value of volume fraction (α). Cells filled with air and liquid have the value of α equal to 0 and 1, respectively. Whereas, the cells

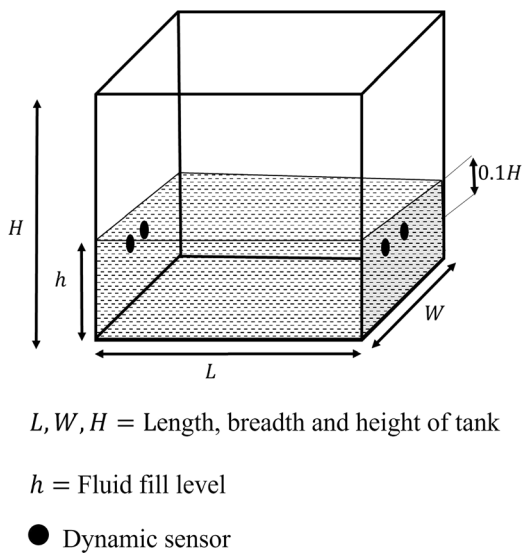

Fig. 2 Location of dynamic sensors on the tank walls for a given fill level

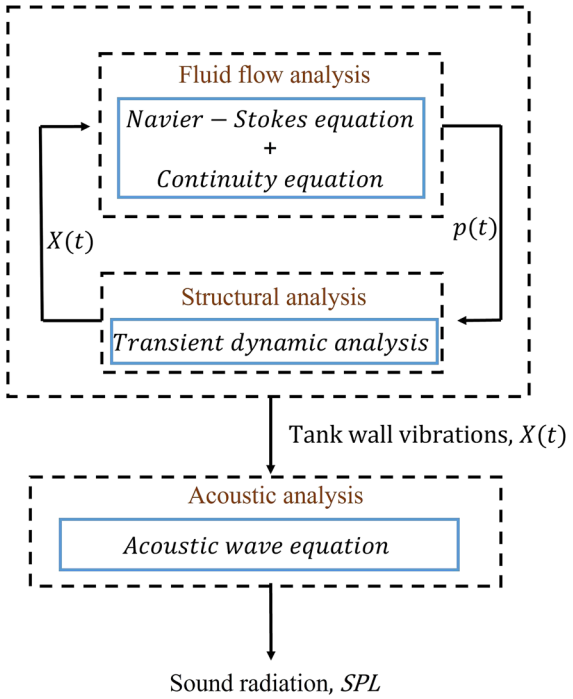

Fig. 3 Flowchart of the numerical methodology to simulate the hit noise

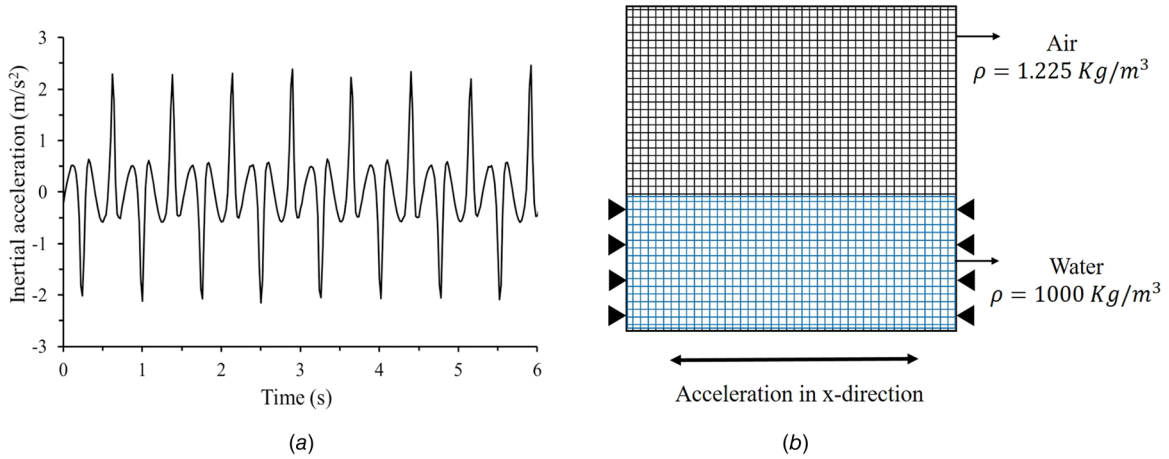

(*a*) (*b*)

Fig. 4 (*a*) Inertial acceleration for 20% fill level at $1f_s$ excitation and (*b*) schematic of the fluid domain in the numerical analysis

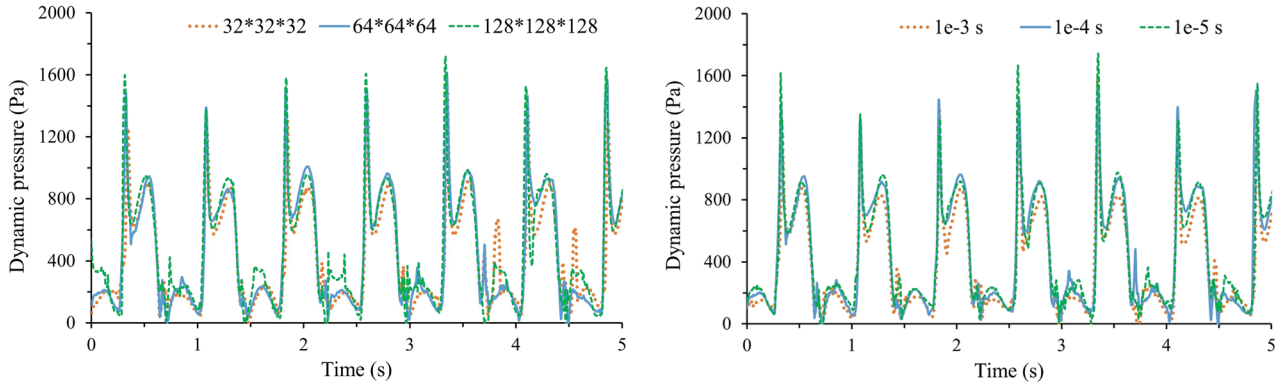

(*a*) (*b*)

Fig. 5 Time history of dynamic pressure at 0.1 H below the free surface to show the convergence study of (*a*) grid size and (*b*) time-step size

with a liquid interface have the value of α between 0 and 1. In the cells with fluid interface, the properties of the cell are given by the linear summation of the properties of the two fluids in the ratio of their respective volume fractions as shown in Eq. (3)

$$\rho = \rho_f \alpha + \rho_g (1 - \alpha) \tag{3a}$$

$$\mu = \mu_f \alpha + \mu_g (1 - \alpha) \tag{3b}$$

The motion of the fluid free surface in a two-phase domain is governed by the advection equation given as

$$\frac{\partial \alpha}{\partial t} + \frac{\partial \alpha \bar{u}_i}{\partial x_j} = 0 \tag{4}$$

The VOF advection equation is solved along with the equations of mass and momentum conservation equations to attain a coupling between the velocity field and fluid distribution and, thus, trace the fluid interface.

The time-averaging of the mass and momentum conservation equations results in the fluxes like Reynold's stress, turbulent diffusion, etc. These fluxes are expressed as mean flow properties by the turbulence models. Therefore, it is important to incorporate an appropriate turbulence model into the computational methodology for the accurate simulation of a fluid flow. $k - \epsilon$ turbulence model is chosen for this study. It employs equations for the kinetic energy of the fluctuation motion (k) and the kinematic rate of energy dissipation (ε).

From the Eqs. (2) and (3), it can be observed that the accuracy of the simulation also depends on the spatial discretization of the fluid domain and the temporal discretization of the transient term. The transient term in the advection equations is discretized using a first-order implicit scheme. Therefore, apart from the choice of turbulence model, the size of mesh and time-step also influences the accuracy of the fluid flow analysis. This can be done by performing convergence studies with respect to each of these parameters. The convergence studies are performed for the 20% fill level at an excitation frequency of $1f_s$. As the excitation is at the sloshing natural frequency (f_s), the fluid flow inside the tank will be chaotic with dominant fluid–structure interactions. Therefore, the choice of parameters for the appropriate simulation of this case may be sufficient for other conditions in which fluid–structure interactions are dominant.

Figures 5(*a*) and 5(*b*) shows the time history of dynamic pressures at a level of $0.1H$ below the free surface, for the chosen test case with different grid sizes and time-steps, which is represented

Table 1 Summary of the results of grid dependence study

Description	Grid size	RMS pressure (Pa)	Relative change (δ)
Coarse	$32 \times 32 \times 32$	537	$p = 1.95$
Medium	$\mathbf{64 \times 64 \times 64}$	**586**	**8.36%**
Fine	$128 \times 128 \times 128$	599	2.17%

The grid size and time-step values chosen for further fluid analysis are highlighted in bold text.

Table 2 Summary of the results of time-step dependence study

Description	Time-step size (Δt)	RMS pressure (Pa)	Relative change (δ)
Large	$\times 10^{-3}$ s	520	$p = 1.41$
Medium	**1×10^{-4} s**	**596**	**12.8%**
Fine	1×10^{-5} s	599	0.5%

The grid size and time-step values chosen for further fluid analysis are highlighted in bold text.

as its root-mean-square (RMS) value in Tables 1 and 2. All computations for the convergence studies are done for a time-period of 5 s (seven oscillation periods) and the RMS value is calculated over the time history of the dynamic pressure. Tables 1 and 2 also present the relative difference (δ) between two grid and time-step size levels considered. The relative difference is calculated as $\delta = (\varphi_{coarser} - \varphi_{finer})/\varphi_{coarser}$, where $\varphi_{coarser}$ and φ_{finer} are the numerical solutions of coarser and finer levels of the two considered grids (or) larger and smaller time-steps. It can be observed from Table 1 that the relative difference between the coarser and the medium grids is significantly high compared to the relative change between the medium and the fine grids. Similar observation can be made from time-step dependence shown in Table 2. Therefore, putting in view the computational expense, grid size of $64 \times 64 \times 64$ and time-step size of 1×10^{-4}s are chosen for the study. Tables 1 and 2 also show the estimated order of accuracy (p) which is defined as $p = \ln[(\varphi_{medium} - \varphi_{coarse})/(\varphi_{fine} - \varphi_{medium})]/\ln(r)$, where φ_{coarse}, φ_{medium}, and φ_{fine} are the numerical solutions of coarse, medium, and fine levels, respectively, and r is the refinement ratio. Though spatial and temporal terms of the governing equation are discretized using the second-order and first-order accurate schemes, the value of p in Tables 1 and 2 indicates that the order of accuracy for the present computational method is between one and two. This is in line with other numerical studies on sloshing [28].

The loading on the tank walls due to fluid interaction results in their vibration. This further induces vibrations into the surrounding air causing hit noise. Therefore, it is important to predict the structural response for the loading due to a given flow condition. For this purpose, the pressure distribution on the tank walls is transferred to the structural domain as a loading condition after every time-step.

3.2 Structural Analysis. A three-dimensional finite element model of the rectangular tank of chosen dimensions is created using shell elements (SHELL181) and is fixed at the bottom. The material of the tank is acrylic, and its mass density (ρ_s), Young's modulus (E_s), and Poisson's ratio (ν_s) are 1100 kg/m^3, 2.1 GPa, and 0.4, respectively. Fluid is modeled inside the tank using acoustic fluid elements (FLUID30). The interaction between the structure and the fluid at the interfaces is accounted for through a coupling of their respective translational DOFs in the normal direction. This is to account for the inertia loading due to liquid mass on the tank walls. The density (ρ_f) and bulk modulus (K_f) of the fluid are 1000 kg/m^3 and 2.2 GPa, respectively, which implies that the speed of sound in the fluid (C_f) is about 1500 m/s. Based on the boundary conditions and appropriate discretization of the domain, the mass [**M**] and the stiffness [**K**] matrices are assembled using the standard FEM procedures. The schematic of the structural domain along with the boundary conditions is shown in Fig. 6(*a*).

The effect of the fluid fill on the tank dynamics can be understood through modal analysis which gives an insight into the variation of tank modal characteristics with fill level. Figure 6(*b*) shows a comparison between the experimental and numerical results of the modal analysis of the tank at different fill levels. It can be noticed that the natural frequency of the tank decreases with an increase in the fill level. This indicates that the inertia effect of the fluid is dominant in the tank.

The transient structural response of the tank walls for the fluid impacts during sloshing is governed by the equation of motion as given by the following equation:

$$[\mathbf{M}]\{\ddot{\mathbf{X}}\} + [\mathbf{C}]\{\dot{\mathbf{X}}\} + [\mathbf{K}]\{\mathbf{X}\} = \{\mathbf{F_p}\} \tag{5}$$

where [**C**] is the damping matrix and {**X**} is the nodal displacement vector. {$\mathbf{F_p}$} is the transient force acting on the nodes of tank walls due to fluid loading during sloshing. It is obtained by integrating the fluid pressure over the area of the elements of the tank wall surface and distributing the resulting load equally among its nodes. The fluid pressure load on tank walls is obtained from the fluid solver at every time-step as it is weakly coupled with the structural solver through a commercial interface software (MPCCI) [29]. Based on the grid convergence study performed during the tank modal analysis, the discretization of the structural domain is chosen as $25 \times 25 \times 25$.

3.3 Coupling Process. The flowchart of the weak coupling process is shown in Fig. 7. In weak coupling, the governing equations of each domain are solved by their respective solvers separately and a few variables are exchanged between them. Here, the pressure on the tank walls due to fluid interactions is transferred to the structural domain as a loading condition and the tank wall displacements due to this pressure loading are transferred to the fluid domain as a new boundary condition. This exchange process is done for every time-step only after the convergence of the displacement and pressures is attained. The tank wall vibrations

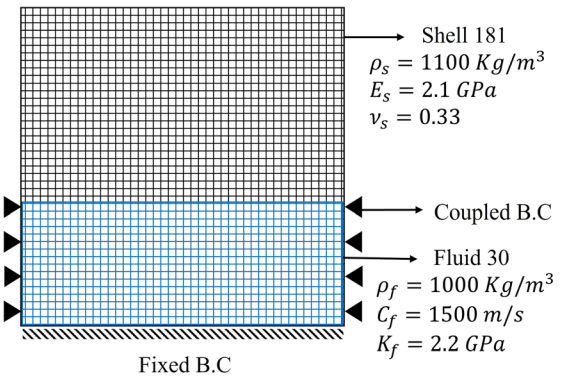

(*a*)

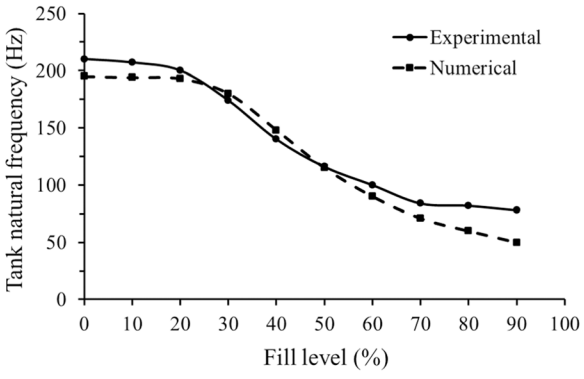

(*b*)

Fig. 6 (*a*) Schematic of the structural domain in the numerical analysis and (*b*) effect of fill level on the modal characteristics of the tank

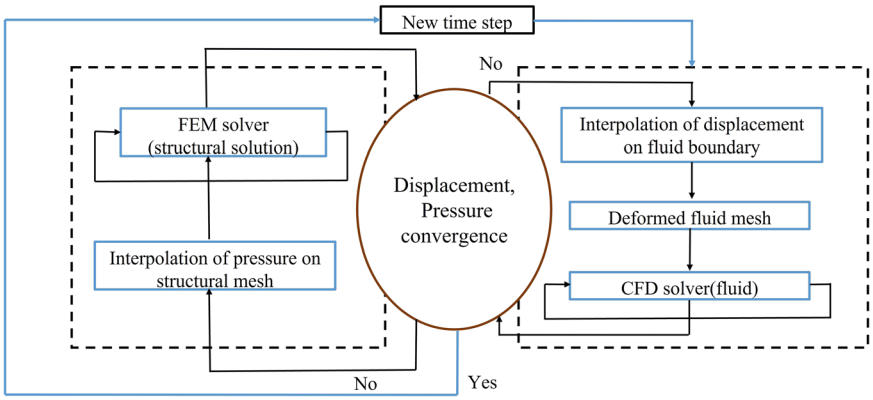

Fig. 7 Flowchart of the coupling process between the fluid and structural solvers

obtained in the form of displacements are applied as a boundary condition to the acoustic domain in the transient FEM analysis.

3.4 Acoustic Domain. The schematic of the acoustic domain is shown in Fig. 8. The tank is treated as to be embedded in an acoustic domain (Ω_A). The vibrations at the tank boundary (S_B) due to fluid loading cause pressure perturbations in the acoustic domain resulting in the sound propagation. The fluid in the acoustic domain is assumed to be incompressible, inviscid, isentropic, and perturbations in density, particle velocity, and pressure about their respective mean values are considered to be small.

A transient exterior acoustic problem can be modeled as a boundary value problem governed by the wave equation with Dirichlet (or) Neumann boundary conditions at the tank boundary (S_B) and appropriate radiation boundary condition at the truncation of the acoustic domain (S_R).

The sound propagation in the fluid medium around the tank is governed by the linear acoustic wave equation which is given as

$$\nabla^2 p'(x,y,z,t) = \frac{1}{c_0^2}\frac{\partial^2 p'(x,y,z,t)}{\partial t^2} \tag{6}$$

where ∇^2 is the Laplace operator, $p'(x,y,z,t)$ is the acoustic pressure at time t, c_0 is the speed of sound in the acoustic medium. The boundary conditions on the S_B are given by

$$\frac{\partial p'}{\partial n} = -\rho\frac{\partial u_n(t)}{\partial t} \tag{7}$$

where n is the outward normal to S_B, ρ is the density of the fluid in the acoustic domain and $u_n(t)$, $\dot{u}_n(t)$ are the normal velocity and acceleration on S_B. The hemispherical boundary (S_R) of the acoustical domain is applied with Sommerfeld's radiation condition which is given as

$$\lim_{r\to\infty} r\left(\frac{\partial p'}{\partial r} + \frac{1}{c_0}\frac{\partial p'}{\partial t}\right) = O\left(\frac{1}{r}\right) \tag{8}$$

where r is the radial outward distance. It specifies that there are only waves that are radiating outward from the source toward the boundary S_R and no waves coming from the infinity. As the tank is fixed to the carriage, the acoustic domain (Ω_A) is considered to be hemispherical with the normal velocity (v_n) of its base (S_F) to be zero. The acoustic domain is discretized with six elements per wavelength of the maximum frequency of interest.

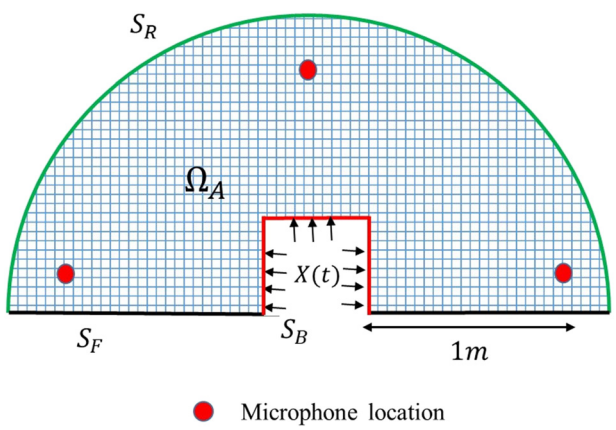

Fig. 8 Schematic of the acoustic domain in the numerical analysis

4 Results and Discussion

The proposed numerical methodology is used to predict the radiated hit noise for different fill levels. The methodology is validated for its accuracy against the experimental results in each domain individually.

4.1 Fluid Domain. The parameters chosen from the convergence studies are used to simulate the sloshing phenomena for 20% fill level at the excitation of $1f_s$(80 rpm), i.e., 1.35 Hz. As the excitation is equal to the sloshing resonance, it results in a chaotic sloshing in the tank with predominant fluid–structure interactions. The numerical results of the fluid domain are validated in terms of fluid free surface profiles and tank wall loading in time and frequency domains, as done in Ref. [9]. Figure 9 shows the comparison of fluid flow between experimental and numerical studies for this case. In this, the free surface profiles at three different time instants representing—(i) the motion of surface wave from the rear wall to the front wall at the instant of 0.44 s in Figs. 9(*a*) and 9(*d*), (ii) elevation of the liquid column along the front tank wall due to fluid–structure interaction at the instant of 0.65 s in Figs. 9(*b*) and 9(*e*), and (iii) the motion of surface wave from the front wall to the rear wall at the instant of 0.82 s in Figs. 9(*c*) and 9(*f*). In the fluid zone, air and water are differentiated using VOF method. VOF is between 0 and 1. Zero represents only air and one represents only water. Thus, from Fig. 9, it can be observed that the fluid flow is appropriately simulated in the numerical study.

The comparison of the experimentally and numerically obtained fluid loading on the tank walls is shown in Fig. 10 in the form of dynamic pressure variation w.r.t time and its frequency representation. The peaks in Fig. 10(*a*) represent the fluid impact on the tank wall and have a time gap corresponding to the excitation frequency. It can be noticed that the pressure variation is appropriately captured by the numerical model in terms of magnitude and occurrence of events. This is supported by Fig. 10(*b*)

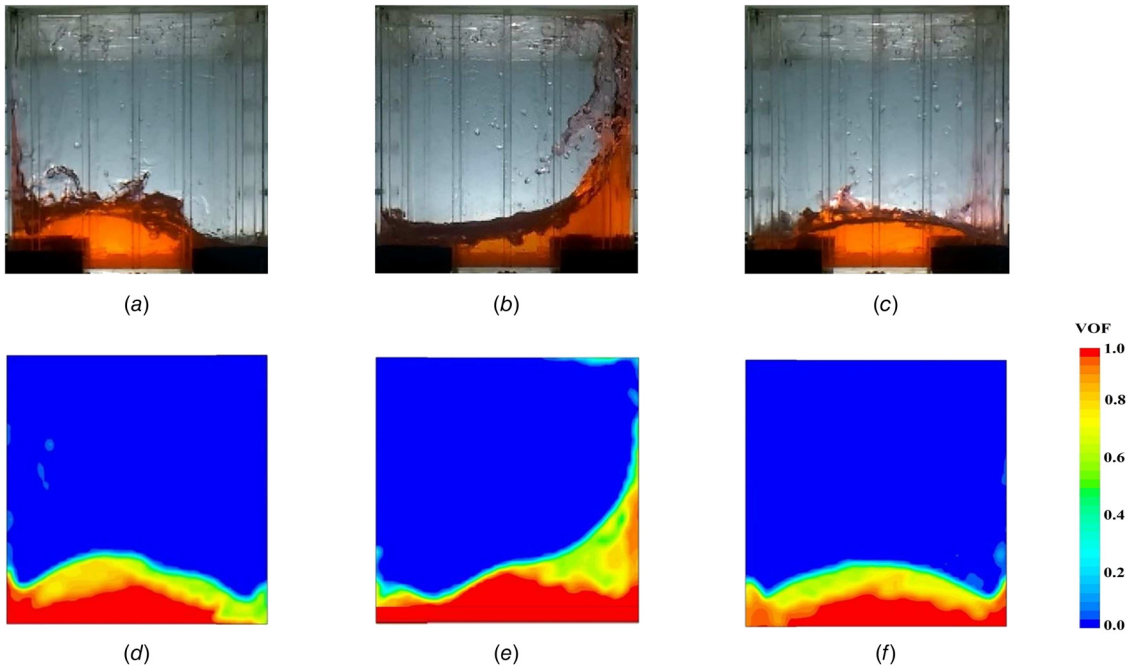

Fig. 9 Comparison of fluid flow between the experimental (top row) and numerical study (bottom row) for 20% fill level at $1f_s$ (80 rpm) excitation for three different time instants (*a* and *d*) 0.44 s, (*b* and *e*) 0.65 s, and (*c* and *f*) 0.82 s

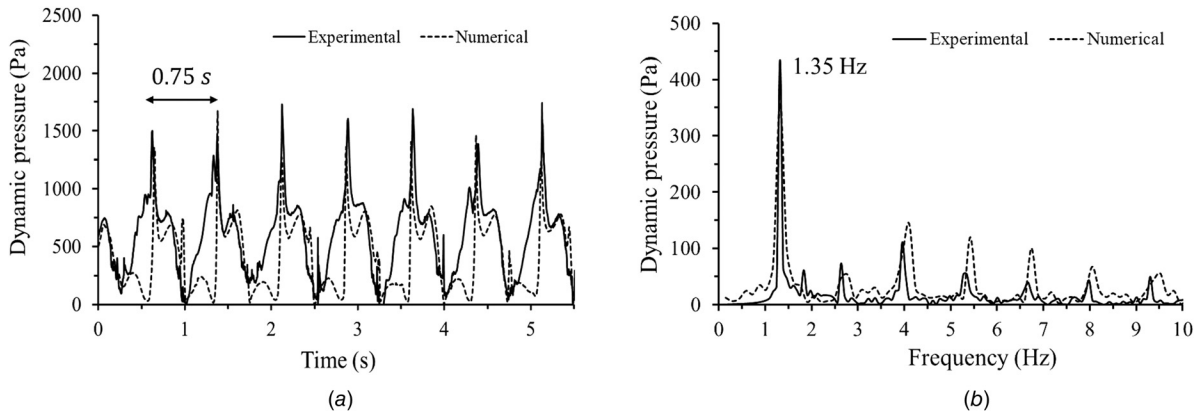

Fig. 10 (*a*) Variation of dynamic pressure with respect to time and (*b*) FFT of the dynamic pressure for 20% fill level at $1f_s$ (80 rpm) excitation

which shows the spectrum of dynamic pressure loading on the tank walls from experimental and numerical studies. It can be observed that the fundamental frequency of the dynamic pressure variation is well matched between experiment and numerical studies. However, deviations are observed at higher frequencies. The amplitude at higher frequencies is significantly lower than the fundamental frequency. Thus, from Figs. 9 and 10 it can be understood that for the chosen mesh size, time-step size, and turbulence model, the proposed numerical model is able to appropriately simulate the sloshing phenomena for the conditions of dominant fluid–structure interactions.

The flow regime of dominant fluid–structure interactions is simulated for three different fill levels, 20%, 40%, and 60%, by imposing excitations at their corresponding $0.75f_s$ and $1f_s$ frequencies. The numerically computed dynamic pressures in these test cases are compared with their respective experimental values in Fig. 11. From this, it can be noticed that the numerical model is able to appropriately predict the loading on the tank walls due to fluid impacts during sloshing.

4.2 Structural and Acoustic Domains. As the fluid and structural solvers are weakly coupled, the dynamic pressures on the tank walls due to fluid loading are transferred to the structural domain at every time-step. For this loading, the structural response is estimated in the form of tank wall vibrations. These tank wall vibrations result in hit noise. The radiated hit noise is predicted through transient acoustic FEM analysis. The vibrations are imposed as input on the surface of the acoustic domain adjacent to the tank. In the experimental study, the tank wall response is measured in the form of dynamic acceleration. The measurement locations are on the front and rear tank walls at a distance of $0.1H$ below the undisturbed fluid domain of the free surface for any given fill level. The sloshing noise is measured using microphones positioned at a distance of 1 m from the front and top tank walls.

Figures 12(*a*) and 12(*b*) shows the experimentally and numerically obtained vibration response on the front tank wall for 20% fill level at $1f_s$ excitation. In the experimental study, the maximum vibration response is occurring at a frequency of 212 Hz, whereas

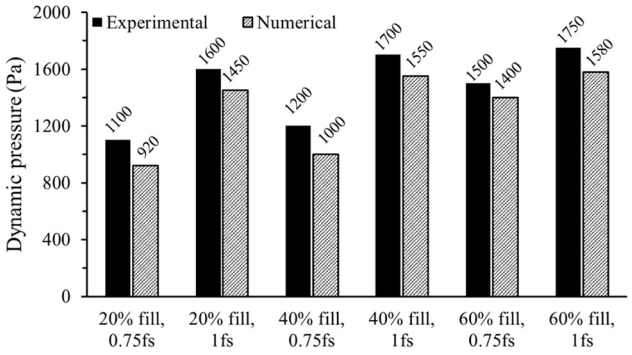

Fig. 11 Comparison of experimentally and numerically obtained maximum magnitudes of dynamic pressures for 20%, 40%, and 60% fill levels at their respective 0.75f_s and 1f_s excitations

it is 208 Hz in the numerical analysis. A similar response is observed in the sound pressure levels also, as can be seen in Figs. 12(*c*) and 12(*d*). This deviation in the frequencies of maximum response can be noticed for 40% and 60% fill levels also from their corresponding experimental and numerical vibration responses and sound pressure levels shown in Figs. 13 and 14, respectively. This deviation can be attributed to the effect of joints of the tank used in the experiments and the inhomogeneity in its material properties. Also, in the experiments, clamps are used at the four corners of the tank to tightly fix it to the wooden platform. This clamped condition is approximated as a fixed condition at the bottom of the tank in the structural analysis and could be the possible reason for the deviation between experimental and numerical results.

In the experiments, the traverse of the tank over the guide vanes by the slider-crank mechanism at higher speeds led to the vibration of the mounting base. This could have led to the presence of considerable energy below the peak frequency and the spread of sidebands at lower frequencies in the dynamic acceleration spectrum. This phenomenon could not have been captured in the simulations. Also, in the experiments, at resonance condition, though the hit noise due to fluid–structure interactions dominates, there are other noise sources like splash due to wave breakage. Such noise is not captured in the simulations which used vibro-acoustic methodology for the prediction of hit noise. This could be the reason for the difference in the spectra of sound pressure levels (SPL) from experiments and simulations, though the peaks are closely matching.

Figure 15 shows the comparison of experimentally and numerically obtained sound pressure levels for 20%, 40%, and 60% fill levels at their respective 0.75f_s and 1f_s excitations. It can be noticed that the prediction by the numerical model has followed

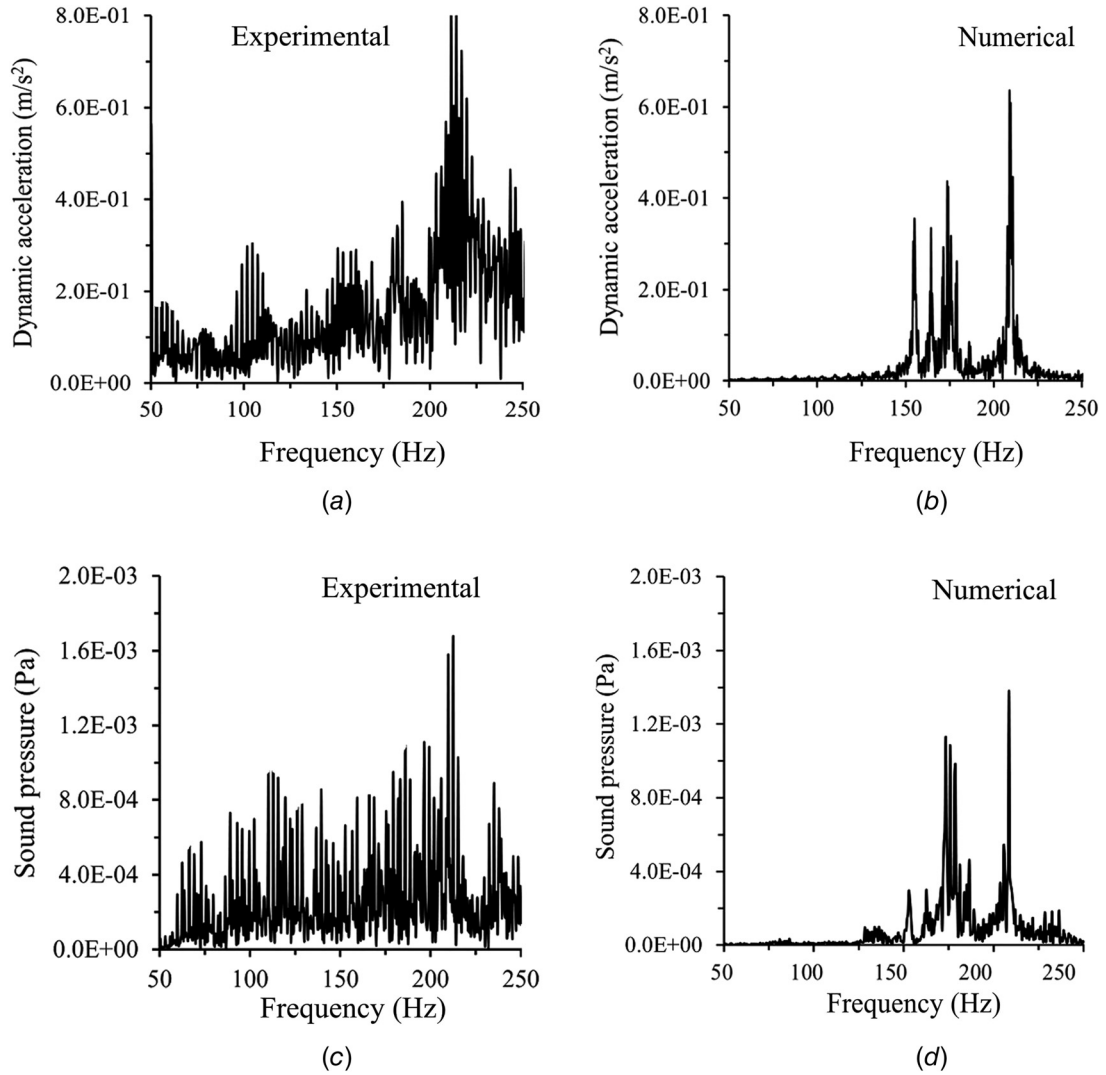

Fig. 12 Comparison of (*a* and *b*) structural and (*c* and *d*) acoustic responses from experimental and numerical studies for the 20% fill level at 1f_s (80 rpm) excitation

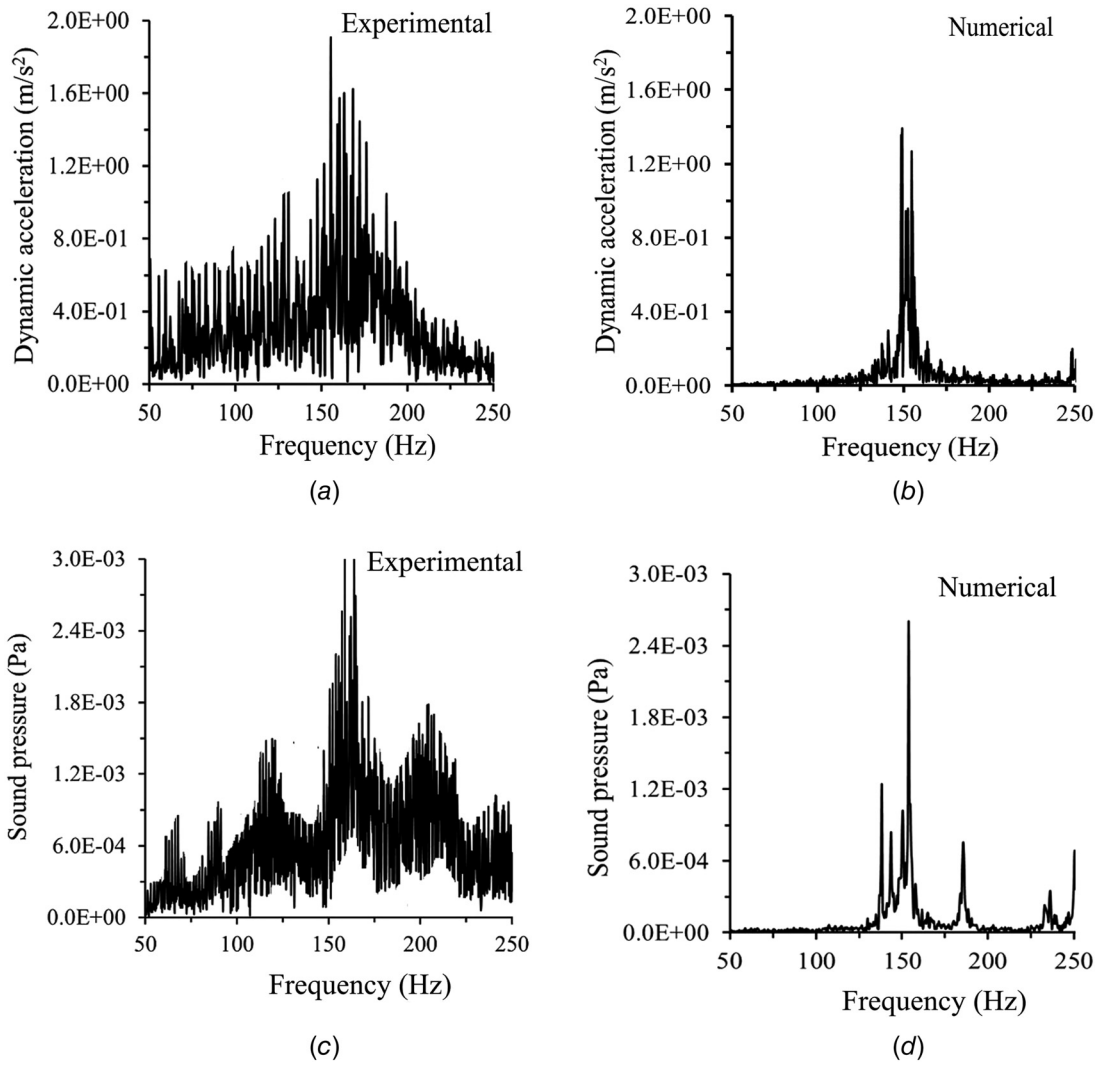

Fig. 13 Comparison of (*a* and *b*) structural and (*c* and *d*) acoustic responses from experimental and numerical studies for the 40% fill level at 1f_s (100 rpm) excitation

the trend of the experimental results. It can be observed that for test cases of 20% fill at 0.75f_s, 1f_s excitations and 40% fill at 0.75f_s excitation, the prediction of SPL is within the limit of 3 *dB*. For the rest of the test cases, the difference is higher. It is because of the occurrence of fluid–fluid interactions due to wave breakages for those fill levels at the excitations specified in Fig. 15. Therefore, it can be understood that the numerical methodology proposed in this paper could appropriately predict the hit noise generated due to fluid–structure interactions during sloshing.

5 Conclusions

The noise generated during sloshing due to the interaction of the fluid with the structure is termed hit noise. The generation of hit noise is a multi-physics phenomenon that involves the interaction among fluid, structural and acoustic domains. Therefore, appropriate simulation of the phenomena happening in each of the involved physical domains is key to the accurate prediction of the hit noise. This paper presents a multi-physics numerical methodology for this purpose and is validated with experimental results in each physical domain, individually.

The fluid flow regime in which the hit noise is dominant is created in a rectangular tank for different fill levels, in the experimental study by imposing the longitudinal periodic excitation at different frequencies. Various dynamic events are captured during the experiments and are used to validate the proposed numerical methodology. The dynamic parameters such as inertial acceleration, fluid pressure, tank wall vibrations, and radiated sound pressure levels are measured with proper instrumentation. The experimentally measured inertial acceleration of the tank is imposed as a longitudinal momentum to the fluid domain for the appropriate simulation of the fluid flow.

The fluid and the structural domains are weakly coupled in order to predict the tank structural response due to the fluid impacts on the tank walls under given conditions of fill level and excitation frequency. These tank wall vibrations induce perturbations into the surrounding fluid medium. Thus, in the acoustic analysis, they are given as boundary condition at the interface of the tank and the surrounding acoustic medium, and the sound propagation is predicted by solving the wave equation. The proposed methodology is validated in each physical domain, individually. A parametric study has been conducted to understand the role of fill level and excitation frequency in hit noise generation. The predicted parameters of fluid flow, fluid loading, tank structural response, and radiated sound are in good agreement with their respective experimental measurements. This study is restricted to a lab-scale demonstration tank. Future work will include investigations on full scale automotive tanks so that scaling laws can be investigated which can in turn help is faster design of such tanks. This study is restricted to a lab-scale demonstration

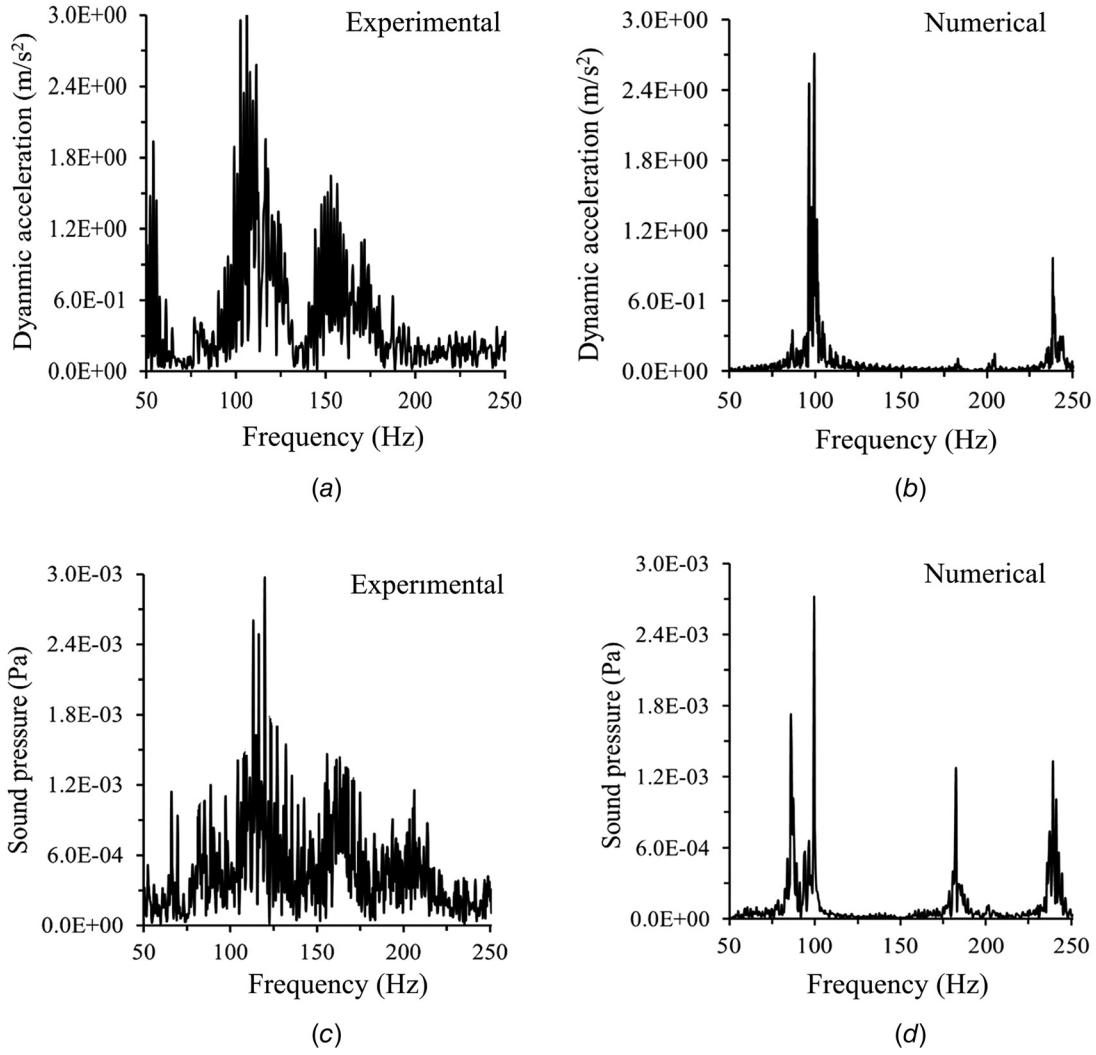

Fig. 14 Comparison of (*a* and *b*) structural and (*c* and *d*) acoustic responses from experimental and numerical studies for the 60% fill level at 1f_s (106 rpm) excitation

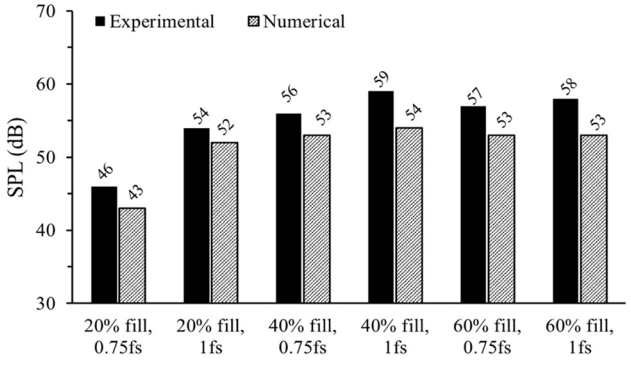

Fig. 15 Comparison of experimentally and numerically obtained maximum SPL for 20%, 40%, and 60% fill levels at their respective 0.75f_s and 1f_s excitations

tank. Future work will include investigations on full scale automotive tanks so that scaling laws can be investigated which can in turn help is faster design of such tanks.

Funding Data

- Indian Institute of Technology Hyderabad and Ministry of Education, Government of India.

Data Availability Statement

The datasets generated and supporting the findings of this article are obtainable from the corresponding author upon reasonable request.

References

[1] Ibrahim, R. A., 2005, *Liquid Sloshing Dynamics: Theory and Applications*, Cambridge University Press, Cambridge, UK.

[2] Wachowski, C., Biermann, J., and Schala, R., 2010, "Approaches to Analyse and Predict Slosh Noise of Vehicle Fuel Tanks," 24th International Conference of Noise and Vibration Engineering (ISMA2010), Leuven, Belgium, Sept. 20–22, pp. 4399–4414.

[3] Golla, S. T., and Venkatesham, B., 2021, "Experimental Study on the Effect of Centrally Positioned Vertical Baffles on Sloshing Noise in a Rectangular Tank," Appl. Acoust., **176**, p. 107890.

[4] Rebouillat, S., and Liksonov, D., 2010, "Fluid–Structure Interaction in Partially Filled Liquid Containers: A Comparative Review of Numerical Approaches," Comput. Fluids, **39**(5), pp. 739–746.

[5] Chen, Y., and Xue, M.-A., 2018, "Numerical Simulation of Liquid Sloshing With Different Filling Levels Using Openfoam and Experimental Validation," Water, **10**(12), p. 1752.

[6] Eswaran, M., Saha, U., and Maity, D., 2009, "Effect of Baffles on a Partially Filled Cubic Tank: Numerical Simulation and Experimental Validation," Comput. Struct., **87**(3–4), pp. 198–205.

[7] Vaishnav, D., Dong, M., Shah, M., Gomez, F., and Usman, M., 2014, "Investigation and Development of Fuel Slosh Cae Methodologies," SAE Int. J. Passen. Cars-Mech. Syst., **7**(1), pp. 278–288.

[8] Liu, D., Tang, W., Wang, J., Xue, H., and Wang, K., 2016, "Comparison of Laminar Model, RANS, LES and VLES for Simulation of Liquid Sloshing," Appl. Ocean Res., **59**, pp. 638–649.

[9] Kabiri, M. M., Nikoomanesh, M. R., Danesh, P. N., and Goudarzi, M. A., 2019, "Numerical and Experimental Evaluation of Sloshing Wave Force Caused by Dynamic Loads in Liquid Tanks," ASME J. Fluids Eng., **141**(11), p. 111112.
[10] Vaziri, N., Chern, M.-J., and Borthwick, A. G., 2015, "Effects of Base Aspect Ratio on Transient Resonant Fluid Sloshing in a Rectangular Tank: A Numerical Study," Ocean Eng., **105**, pp. 112–124.
[11] Brizzolara, S., Savio, L., Viviani, M., Chen, Y., Temarel, P., Couty, N., Hoflack, S., Diebold, L., Moirod, N., and Iglesias, A. S., 2011, "Comparison of Experimental and Numerical Sloshing Loads in Partially Filled Tanks," Ships Offshore Struct., **6**(1–2), pp. 15–43.
[12] Liu, D., and Lin, P., 2008, "A Numerical Study of Three-Dimensional Liquid Sloshing in Tanks," J. Comput. Phys., **227**(8), pp. 3921–3939.
[13] Moretti, F. L., Silveira, M. E., Lamin, P. C., Brito, J. N., and Pockszevnicki, B. C., 2014, "Numerical and Experimental Evaluation of Sloshing in Automotive Fuel Tanks," SAE Paper No. 2014-360122.
[14] Molin, B., and Remy, F., 2013, "Experimental and Numerical Study of the Sloshing Motion in a Rectangular Tank With a Perforated Screen," J. Fluids Struct., **43**, pp. 463–480.
[15] Frosina, E., Senatore, A., Andreozzi, A., Fortunato, F., and Giliberti, P., 2018, "Experimental and Numerical Analyses of the Sloshing in a Fuel Tank," Energies, **11**(3), p. 682.
[16] Zhang, E., 2020, "Numerical Research on Sloshing of Free Oil Liquid Surface Based on Different Baffle Shapes in Rectangular Fuel Tank," Proc. Inst. Mech. Eng., Part D J. Autom. Eng., **234**(2–3), pp. 363–377.
[17] Aus der Wiesche, S., 2003, "Computational Slosh Dynamics: Theory and Industrial Application," Comput. Mech., **30**(5–6), pp. 374–387.
[18] Cruchaga, M. A., Ferrada, C., Márquez, N., Osses, S., Storti, M., and Celentano, D., 2016, "Modeling the Sloshing Problem in a Rectangular Tank With Submerged Incomplete Baffles," Int. J. Numer. Methods Heat Fluid Flow, **26**(3/4), pp. 722–744.
[19] De Man, P., and Van Schaftingen, J.-J., 2012, "Prediction of Vehicle Fuel Tank Slosh Noise From Component-Level Test Data," SAE Paper No. 2012-01-0215.
[20] Kamei, M., Hanai, J., Fukasawa, W., and Makino, T., 2007, "Establishment of a Method for Predicting and Confirming Fuel Tank Sloshing Noise," SAE Paper No. 2007-01-1538.
[21] Balthy, M., Jain, C. P., Makana, M., and Katti, R., 2011, "Development of a Quantification Methodology for Slosh Noise Associated With Dynamic Fuel Flow Behavior in Passenger Car Tank," SAE Paper No. 2011-28-0089.
[22] Park, J.-S., Choi, S.-C., and Hong, S.-G., 2011, "The Prediction of Fuel Sloshing Noise Based on Fluid-Structure Interaction Analysis," SAE Int. J. Passen. Cars-Mech. Syst., **4**(2), pp. 1304–1310.
[23] Roh, W.-J., Cho, S.-H., and Park, J. I., 2005, "Simulation of Sloshing in Fuel Tanks and Parametric Study on Noise Reduction by Decreasing Impact Pressure," SAE Trans., **114**, pp. 2431–2436.
[24] Li, F., Sibal, S. D., McGann, I. F., and Hallez, R., 2011, "Radiated Fuel Tank Slosh Noise Simulation," SAE Paper No. 2011-01-0495.
[25] Saptoadi, H., 2017, "Suitable Deceleration Rates for Environmental Friendly City Driving," Int. J. Res. Chem., Metall. Civ. Eng., **4**(1), pp. 2–5.
[26] Maurya, A. K., and Bokare, P. S., 2012, "Study of Deceleration Behaviour of Different Vehicle Types," Int. J. Traffic Transp. Eng., **2**(3), pp. 253–270.
[27] Golla, S. T., Mayur, K., Venkatesham, B., and Banerjee, R., 2019, "Experimental Study of Sloshing Noise in a Partially Filled Rectangular Tank Under Periodic Excitation," Proc. Inst. Mech. Eng., Part D J. Autom. Eng., **233**(11), pp. 2891–2902.
[28] Wilson, R. V., Stern, F., Coleman, H. W., and Paterson, E. G., 2001, "Comprehensive Approach to Verification and Validation of Cfd Simulations–Part 2: Application for Rans Simulation of a Cargo/Container Ship," ASME J. Fluids Eng., **123**(4), pp. 803–810.
[29] Fraunhofer, S. C. A. I., 2018, "MpCCI 4.6.0 User Manual," Fraunhofer Institute for Algorithms and Scientific Computing SCAI, Sankt Augustin, Germany.